

# Tissue-engineered dermo-epidermal skin analogs exhibit de novo formation of a near natural neurovascular link 10 weeks after transplantation

Thomas Biedermann · Agnieszka S. Klar ·  
Sophie Böttcher-Haberzeth · Clemens Schiestl ·  
Ernst Reichmann · Martin Meuli

Published online: 21 December 2013  
© Springer-Verlag Berlin Heidelberg 2013

## Abstract

**Purpose** Human autologous tissue-engineered skin grafts are a promising way to cover skin defects. Clearly, it is mandatory to study essential biological dynamics after transplantation, including reinnervation. Previously, we have already shown that human tissue-engineered skin analogs are reinnervated by host nerve fibers as early as 8 weeks after transplantation. In this study, we tested the hypothesis that there is a de novo formation of a “classical” neurovascular link in tissue-engineered and then transplanted skin substitutes.

**Methods** Keratinocytes, melanocytes, and fibroblasts were isolated from human skin biopsies. After expansion in culture, keratinocytes and melanocytes were seeded on dermal fibroblast-containing collagen type I hydrogels. These human tissue-engineered dermo-epidermal skin analogs were transplanted onto full-thickness skin wounds on the back of immuno-incompetent rats. Grafts were analyzed after 3 and 10 weeks. Histological sections were examined with regard to the ingrowth pattern of myelinated and unmyelinated nerve fibers into the skin analogs using markers such as PGP9.5, NF-200, and NF-160. Blood vessels were identified with CD31, lymphatic vessels with Lyve1. In particular, we focused on alignment patterns between nerve

fibers and either blood and/or lymphatic vessels with regard to neurovascular link formation.

**Results** 3 weeks after transplantation, blood vessels, but no nerve fibers or lymphatic vessels could be observed. 10 weeks after transplantation, we could detect an ingrowth of myelinated and unmyelinated nerve fibers into the skin analogs. Nerve fibers were found in close proximity to CD31-positive blood vessels, but not alongside Lyve1-positive lymphatic vessels.

**Conclusion** These data suggest that host-derived innervation of tissue-engineered dermo-epidermal skin analogs is initiated by and guided alongside blood vessels present early post-transplantation. This observation is consistent with the concept of a cross talk between neurovascular structures, known as the neurovascular link.

**Keywords** Human skin analog · Tissue engineering · Blood vessels · Nerve fibers · Innervation · Neurovascular link · Lymphatic vessels

## Introduction

Loss of full-thickness skin is unequivocally accompanied by loss of skin sensibility. Although there is a large spectrum of surgical methods to cover skin defects (transplantation of full-thickness skin, split-thickness skin, biosynthetic skin substitutes, cultured epithelial cells, and combinations thereof), initially there is no sensibility present as nerve fibers migrate only slowly from the wound bed into the transplant [1–6]. Little is known about the chain of events leading to reinnervation, especially since skin appendages such as hair follicles and sweat glands known to provide guidance cues for nerve fibers are also missing [7, 8].

T. Biedermann and A. S. Klar contributed equally to this paper.

T. Biedermann · A. S. Klar · S. Böttcher-Haberzeth ·  
E. Reichmann  
Tissue Biology Research Unit, University Children’s Hospital  
Zurich, Zurich, Switzerland

S. Böttcher-Haberzeth · C. Schiestl · M. Meuli (✉)  
Department of Surgery, University Children’s Hospital Zurich,  
Steinwiesstrasse 75, 8032 Zurich, Switzerland  
e-mail: martin.meuli@kispi.uzh.ch

It is well documented that blood vessels commonly reside alongside peripheral nerves [9]. Interestingly, nerves and vessels influence one another with regard to patterning, branching, development, and regeneration after injury [10–12]. For example, smooth muscle cells surrounding blood vessels secrete artemin, a glial cell-derived neurotrophic factor, which binds the Ret/GFR $\alpha$ 3 receptor of neurons and so guides the nerve fiber to the target organ [13]. In addition, it appears that vascular endothelial cell-derived VEGF-A can control axon cone growth of neurons and guide nerve sprouting along arterial networks via VEGF-receptor 2 signaling [14, 15].

We have recently shown that tissue-engineered and then transplanted dermo-epidermal skin analogs are distinctly vascularized by host blood capillaries after 3 weeks [16]. However, the ingrowth of nerve fibers into the transplant was observed only 8 weeks after transplantation.

We now investigated if the nerve fibers are attracted by and grow alongside the blood vessel network into the transplanted skin analogs and if there is also a topographical relationship between nerve fibers and the lymphatic vessels.

## Materials and methods

### Human skin samples

This experimental study was performed in accordance with the Declaration of Helsinki Principles and after permission by the Ethic Committee of the Canton Zurich. Informed consent was given by parents and/or patients. Human foreskins or skin samples from scalp or abdomen were obtained from patients aged between 1 and 18 years. The skin biopsies were used for isolation of human epidermal keratinocytes, melanocytes, and dermal fibroblasts.

### Isolation and culturing of primary cells

Keratinocytes and fibroblasts were isolated and cultured as described by Biedermann et al. [17]. Melanocytes were isolated and kept in culture as specified by Böttcher-Haberzeth et al. [18].

### Preparation of dermo-epidermal skin analogs

Skin analogs were prepared in six-well cell culture inserts with 3.0  $\mu$ m pore size membranes in a transwell system (BD Falcon, Switzerland) [19]. To generate the dermal compartment, the membranes were covered with

collagen type I hydrogels containing human dermal fibroblasts. Rat tail collagen type I (0.7 ml) (BD Biosciences, Switzerland) was mixed with 0.2 ml chilled neutralization buffer containing 0.15 M NaOH and  $1 \times 10^5$  fibroblasts (passage 1). After polymerization (10 min at room temperature and 20 min at 37 °C), the dermal equivalents were cultured in DMEM containing 10 % FCS for 5 days. Subsequently, keratinocytes and melanocytes (ratio 5:1, passage 1–3) were seeded onto each dermal equivalent at a density of  $4 \times 10^5$  cells. The skin analogs were cultured in SFM (Invitrogen, Switzerland) for 1 week before transplantation. The medium was changed every second day.

### Transplantation of cultured dermo-epidermal skin analogs

The surgical procedure was approved by the local committee for Experimental Animal Research (permission numbers 65/2009, 76/2011). Immuno-incompetent female nu/nu rats, 8–10 weeks old (Harlan Laboratories, Netherlands) were anesthetized prior to operation as previously described [20, 21]. To protect the skin analogs and to prevent wound closure from surrounding rat skin, surgical steel rings (diameter 2.6 cm) were sutured into full-thickness skin defects made on the backs of the rats, using non-absorbable polyester sutures (Ethibond<sup>®</sup>, Ethicon, USA). The transplants were then covered with a silicone foil (Silon-SES, BMS, USA), a polyurethane sponge (Ligasano, Ligamed, Austria), and a tape as wound dressing. Dressing changes and photographic documentations were performed on a weekly basis.

### Analysis of the transplants

After 3 or 10 weeks, animals were killed using CO<sub>2</sub>. Transplants and rat control skin were excised and embedded in OCT compound (Sakura Finetek/Digitana AG, Switzerland). Cryosections were stained with hematoxylin and eosin (Sigma, USA), and mounted within Eukitt (Fluka, Switzerland) for histological analysis. Double immunofluorescence stainings were performed to visualize myelinated and/or unmyelinated rat nerve fibers [ubiquitin carboxyl-terminal hydrolase L1 (PGP9.5, clone 13C4/J3C4, 1:50, Abcam, Germany)], 200 kDa neurofilament (NF200, clone NF01, 1:50, Abcam, Germany), 160 kDa neurofilament (NF160, clone NN18, 1:50, Sigma-Aldrich, Germany), rat vascular endothelial cells [CD31 (clone TDL-3A12, 1:50, BD Pharmingen, Switzerland)], rat lymphatic endothelial cells [Lyve1 (polyclonal, 1:200, Novus Biologicals, UK)], vascular basement membrane protein [Laminin1 + 2 (clone ab7463, 1:500, Abcam,

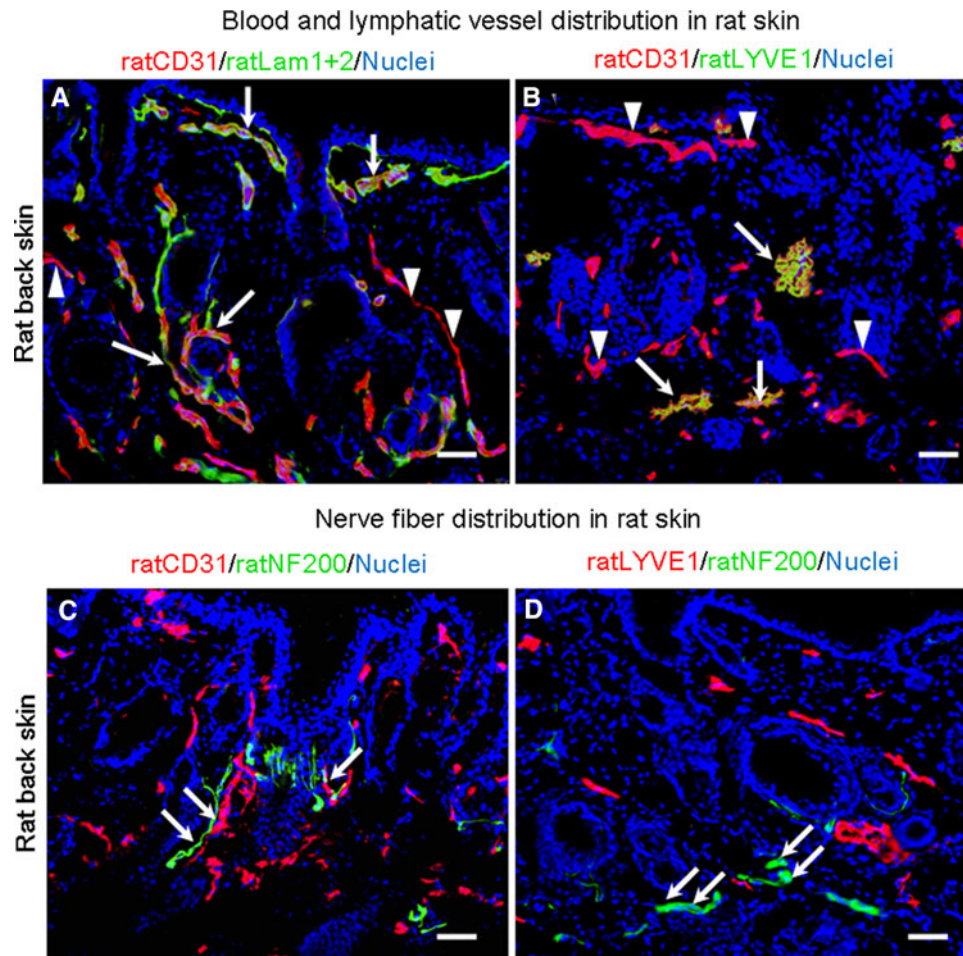


**Fig. 1** Evaluation of blood, lymphatic vessel, and nerve fiber distribution in normal rat back skin. **a** Staining of normal rat skin for CD31 (red) and basement membrane staining for Lam1 + 2 (green). Blood vessels show a double staining with CD31 and Laminin1 + 2 (white arrows); structures staining for CD31 only show lymphatic vessels (white arrowheads). **b** Staining of normal rat skin with LYVE1 (green) and CD31 (red). Lymphatic vessels display a double staining with LYVE1 and CD31 (white arrows); structures

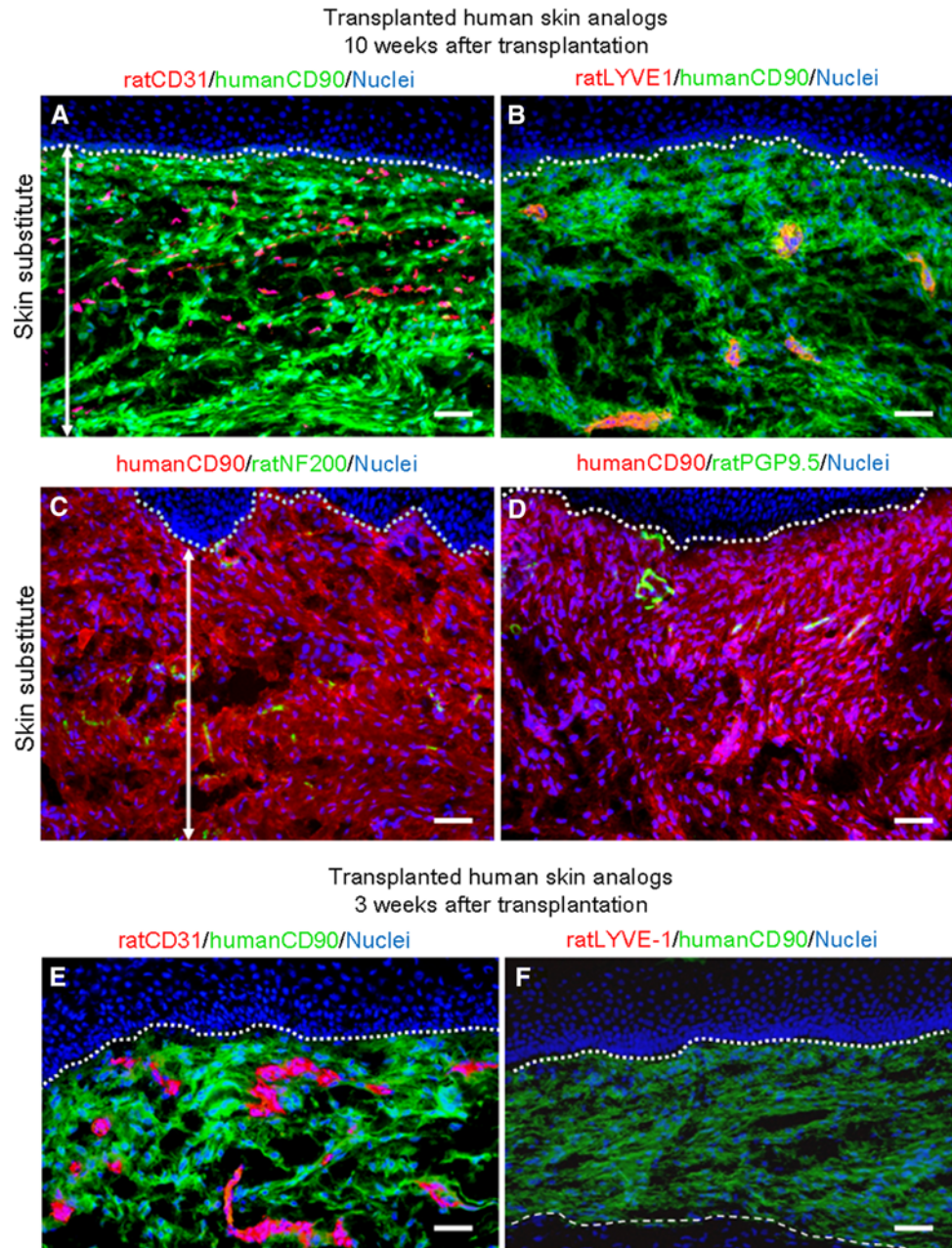
staining for CD31 only show blood vessels (white arrowheads). **c** Staining of blood vessels with CD31 (red) and of nerve fibers with NF200 (green). An alignment between blood vessels and nerve fibers can be detected (white arrows). **d** Staining of lymphatic vessels with LYVE1 (red) and of nerve fibers with NF200 (green). No colocalization between lymphatic vessels and nerve fibers can be noted (white arrows). Cell nuclei are stained with Hoechst (blue). Scale bar for all panels 50  $\mu$ m

Germany)], and human fibroblasts [CD90 (clone AS02, 1:50, Dianova, Germany)]. Cryosections were fixed and permeabilized in acetone/methanol for 5 min at  $-20^{\circ}\text{C}$ , air-dried, and washed  $3\times$  in phosphate-buffered saline (PBS, Invitrogen, Switzerland). Thereafter, sections were blocked in PBS containing 2 % BSA (Sigma, Switzerland) for 30 min. Incubation with the diluted first antibody was performed in blocking buffer for 1 h at room temperature. Afterward, slides were washed three times for 5 min in PBS and blocked for additional 15 min. To visualize the primary antibody, FITC-conjugated polyclonal goat F(ab')<sub>2</sub> fragments directed to mouse immunoglobulins (Dako, Switzerland) were added to the sections. Slides were washed three times for 5 min in PBS and blocked for

additional 15 min. For double immunofluorescence, NF and CD31 primary antibodies were pre-labeled with Alexa 555-conjugated polyclonal goat F(ab')<sub>2</sub> fragments according to the manufacturer's instructions (Zenon Mouse IgG Labeling Kit, Molecular Probes/Invitrogen, Switzerland) and added to the sections. Finally, the slides were incubated for 5 min in PBS containing 1  $\mu\text{g}/\text{ml}$  Hoechst 33342 (Sigma, Switzerland), washed twice for 5 min in PBS, and mounted with Dako mounting solution (Dako, Switzerland).

Pictures of immunofluorescence stainings were taken with a DXM1200F digital camera connected to a Nikon Eclipse TE2000-U inverted microscope. The device is equipped with Hoechst 33342, FITC, and TRITC filter sets

**Fig. 2** Evaluation of host blood and lymphatic vessel distribution as well as host innervation in human tissue-engineered skin analogs 10 weeks after transplantation. **a** Staining of rat blood vessels with CD31 (red) and of human fibroblasts with CD90 (green). **b** Staining of rat lymphatic vessels with LYVE1 (red) and of human fibroblasts with CD90 (green). **c, d** Staining of rat nerve fibers with NF200 and PGP9.5 (green), human dermal fibroblasts are stained with CD90 (red). **e** Staining of rat blood vessels with CD31 (red) and of human fibroblasts with CD90 (green) 3 weeks after transplantation. **f** Staining of rat lymphatic vessels with LYVE1 (red) and of human fibroblasts with CD90 (green) 3 weeks after transplantation. Cell nuclei are stained with Hoechst (blue). The human dermal compartment is marked by a two-sided arrow, the basement membrane is delineated by a dotted line, the lower border of the human compartment by a dashed line. Scale bar for all panels 50  $\mu$ m



(Nikon AG, Switzerland; Software: Nikon ACT-1 vers. 2.70). Images were processed with Photoshop 10.0 (Adobe Systems Inc., Germany).

## Results

Expression of blood- and lymphatic endothelial markers in normal rat skin

Native rat skin from the back was tested for blood- and lymphatic endothelial marker expression (Fig. 1). Skin samples were double-stained for endothelial cells (CD31,

red, Fig. 1a, b) and basement membrane markers (Laminin1 + 2, green, Fig. 1a). In contrast to the CD31 and Laminin1 + 2 positive blood vessels (white arrows, Fig. 1a), the lymphatic vessels were faintly CD31-positive and showed no staining for Laminin1 + 2 (white arrowheads, Fig. 1a).

To further confirm the identity of blood and lymphatic vessels, anti-CD31 staining was combined with LYVE1, which is a marker for lymphatic endothelial cells. As depicted in Fig. 1b, the blood vessels were CD31-positive but LYVE1-negative (white arrowheads), whereas the lymphatic vessels showed a faint CD31 staining and strong LYVE1 expression (white arrows).

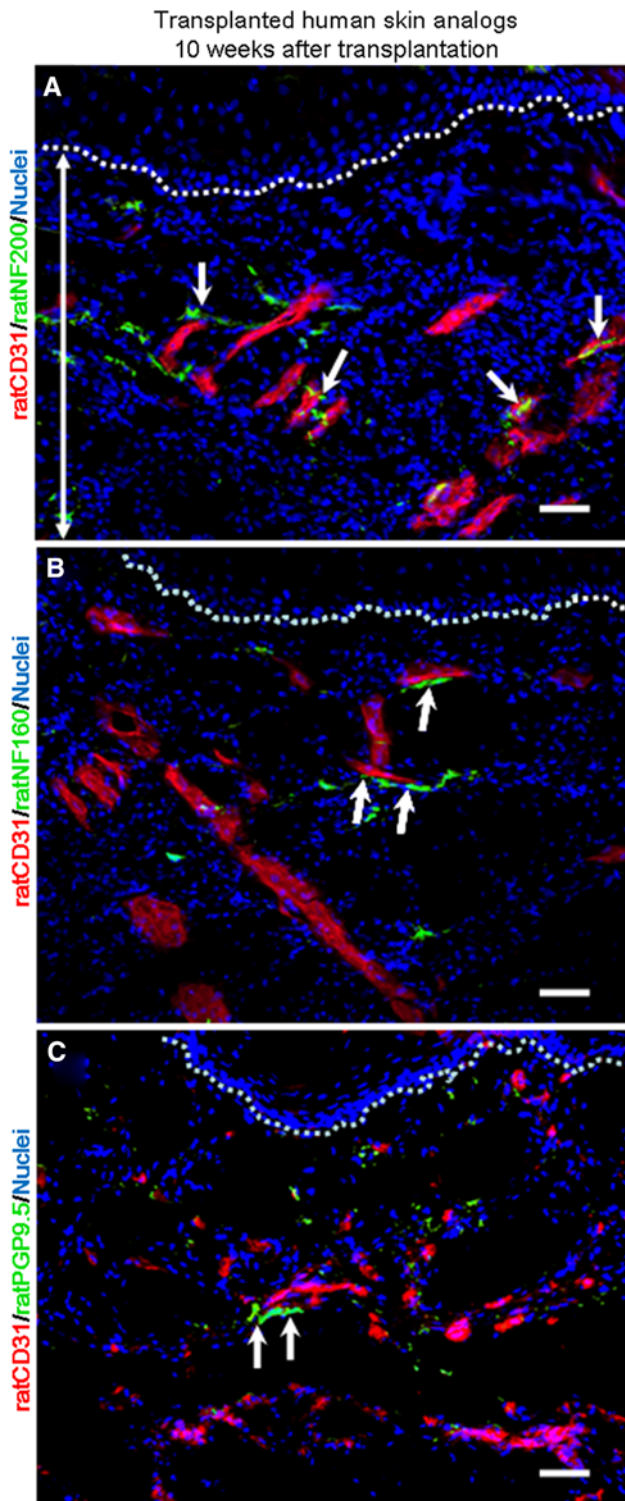


**Fig. 3** Evaluation of host innervation relating to host vascularization in human tissue-engineered skin analogs 10 weeks after transplantation. **a–f** Staining of rat blood vessels with CD31 (red) and of rat nerve fibers with NF200, NF160, and PGP9.5 (green). Cell nuclei are stained with Hoechst (blue). The dermal compartment is marked by a two-sided arrow; the basement membrane is delineated by a dotted line. An alignment between host nerve fibers and blood vessels can be seen in several areas (arrows). Scale bar for all panels 50  $\mu$ m

### Innervation and vascularization pattern of normal rat skin

Native rat skin from the back was co-stained for nerve fiber marker expression using antibodies against NF200 (green), and blood (CD31, red, Fig. 1c) or lymphatic vessels (LYVE1, red; Fig. 1d). We observed that nerve fibers are located in close proximity to blood vessels (white arrows, Fig. 1c), whereas no co-localization of nerve fibers with lymphatic vessels was noted (Fig. 1d).

### Innervation and vascularization pattern of transplanted human tissue-engineered skin analogs

After excision of the human tissue-engineered skin analogs 10 weeks after transplantation, anti rat-CD31 staining showed an abundant capillary network throughout the dermal compartment delineated with a CD90-staining of human fibroblasts (Fig. 2a). In contrast to blood vessels, the LYVE1-positive lymphatic vessels appeared in lower numbers, were irregular in shape, and larger in diameter as compared to blood vessels (Fig. 2b). Host myelinated and unmyelinated rat nerve fibers (green) were detected in the human dermal compartment (CD90, red) by staining for NF200 and PGP9.5 (Fig. 2c, d).

As a control, the presence of established rat blood and lymphatic vessel networks was investigated 3 weeks after transplantation. Blood vessels (CD31, Fig. 2e) occurred abundantly in the human dermal compartment (CD90, green), whereas no lymphatic vessels were detected in the human dermis (Fig. 2f). The earliest ingrowth of lymphatic capillaries into the skin analogs appeared 5 weeks after transplantation (data not shown).

### Pattern of nerve fibers and blood vessels in human tissue-engineered skin analogs

10 weeks post-transplantation, host blood vessels were visualized in the human dermal compartment by anti-CD31 (red) staining. Myelinated nerve fibers were visualized by staining for NF200 (Fig. 3a, b) and NF160 (Fig. 3c, d), while unmyelinated nerve fibers were identified by anti-PGP9.5 staining (Fig. 3e, f). In almost all sections, rat nerve fibers were aligned along blood vessels (white arrows).

### Pattern of nerve fibers and lymphatic vessels in human tissue-engineered skin analogs

10 weeks after transplantation, sections with lymphatic vessels staining positive for LYVE1 were co-stained with nerve fiber markers such as NF200 (Fig. 4a, b), NF160 (Fig. 4c, d), and PGP9.5 (Fig. 4e, f). We observed

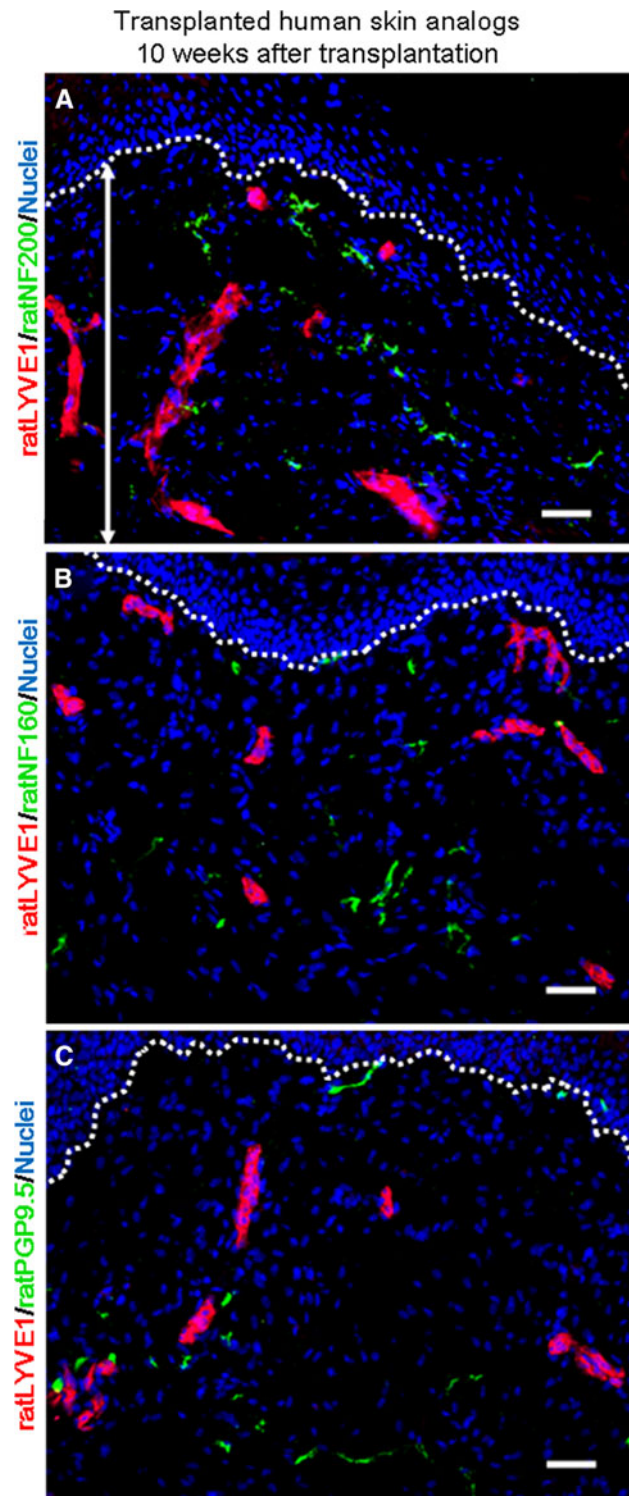


**Fig. 4** Evaluation of host innervation relating to host lymphatic vessels in human tissue-engineered skin analogs 10 weeks after transplantation. **a–f** Staining of rat lymphatic vessels with LYVE1 (red) and of rat nerve fibers with NF200, NF160, and PGP9.5 (green). Cell nuclei are stained with Hoechst (blue). The dermal compartment is marked by a two-sided arrow; the basement membrane is delineated by a dotted line. A vicinity of lymphatic vessels and nerve fibers can be seen, but no alignment. Scale bar for all panels 50  $\mu$ m

lymphatic vessels in vicinity to nerve fibers, but we did not detect any alignment of the structures.

## Discussion

This is an experimental study investigating the question whether host-derived innervation of previously transplanted human tissue-engineered skin analogs is guided alongside host blood or lymphatic vessels. In general, our findings demonstrate a clear cut topographical relationship between blood vessels and nerve fibers, but not between lymphatic vessels and nerve fibers. Thus, our hypothesis that a de novo formation of a typical neurovascular link occurs in tissue-engineered skin grafts after transplantation, proves true.

The dynamics of host blood vessels, lymphatic vessels, and nerve fibers populating transplanted human tissue-engineered skin analogs are fundamentally different. We have shown previously that an established vascular network can be detected as early as 3-week post-transplantation while innervation of the dermal compartment is present only 8-week post-transplantation [16]. Certainly, early vascularization of a transplanted skin analog by capillaries and larger blood vessels is crucial to ensure sustained graft take and long-term survival and has therefore the highest physiological “priority” regarding the establishment of host structures within the transplanted tissue. In contrast, lymphatic vessels and nerve fibers are not indispensable for graft survival during the early stage after transplantation. Therefore, we decided to investigate the skin analogs 10 weeks after transplantation to detect eventual topographical relationships between blood or lymphatic vessels and nerves fibers.

It has been described previously that vascular and nervous networks develop in close proximity during the development, reflecting their mutual dependency [22]. To enable an alignment, the structures need to communicate with each other through signals, a molecular exchange called “neurovascular crosstalk” [23]. Hereby, several guidance molecules, such as artemin, VEGF, or endothelin-3, are secreted from blood vessels and attract nerve fibers along a certain ligand-gradient to establish innervation [12, 14, 15]. On the other hand, guidance signals are also secreted from the peripheral nervous system. For instance, VEGF leads to an attraction and branching of blood vessels as well as to arterial differentiation in the skin [24].

Based on the above-mentioned evidence, we developed our hypothesis that initially non-vascularized and non-innervated laboratory grown skin substitutes develop a kind of physiological perfusion and innervation system over time, a newly formed neurovascular link. Although we did not perform the extremely demanding molecular pathway

studies that the aforementioned ground breaking papers described [12, 14, 15, 22–24], we could convincingly demonstrate that 10 weeks after transplantation a de novo formed neurovascular link was present in the dermal compartment of the perfectly well engrafted skin substitutes. In all specimens examined, there was a typical alignment between blood vessels and nerve fibers as seen in normal neurovascular links. On the other hand, such a relationship could not be seen between lymphatic vessels and blood vessels or nerve fibers.

Clearly, the presence of neurovascular links also means that neurovascular crosstalk must have occurred [23]. In our setting, the initiators of this neurovascular communication have certainly been blood vessels as they are present in these transplants much earlier than nerve fibers.

Also it is a tenable assumption that the vascular network within the grafted area received an intrinsic innervation during the neurovascular link development enabling blood vessels to react to synaptically passed signals that cause vasoconstriction and vasodilatation [25, 26]. It might be interesting to look at this issue in a follow-up study.

Although, our dermo-epidermal skin analogs do not contain only adnexal structures such as hair follicles or sweat glands, a few considerations regarding the potential impact of skin appendages in the context of innervation are worth being made. It has been proposed that integrating such appendages into tissue-engineered skin substitutes could enforce the ingrowth of nerves, as glands and hair follicles are very well vascularized and innervated [7, 8, 27, 28]. It has also been described that the incorporation of Schwann cells or the use of modified scaffolds could promote the innervation of skin analogs [29, 30]. Possibly, the integration of human hair follicles and sweat glands could, besides being a revolutionary step toward engineering normal skin, also improve the velocity and quality of reinnervation of our tissue-engineered dermo-epidermal skin analogs.

Finally, we analyzed the dynamics of lymphatic vessel ingrowth into the transplants. After 10 weeks, we could detect lymphatic vessels and nerve fibers in the dermal compartment. Although lymphatic vessels were found in vicinity of nerve fibers, they did not show an alignment pattern as seen in the neurovascular link.

In conclusion, our data suggest that a de novo formation of a close to natural neurovascular link occurs over a time span of 10 weeks after transplantation of tissue-engineered skin analogs that are initially devoid of any vascular and neural elements.

The fact that there is ingrowth of both, normal neurovascular structures as well as lymphatic vessels into engineered skin grafts has favorable clinical implications in view of the envisioned application of such grafts in human patients.

**Acknowledgments** This work was financially supported by the EU-FP7 project EuroSkinGraft (FP7/2007–2013: Grant Agreement No. 279024), by the EU-FP7 (MultiTERM, Grant Agreement No. 238551) and the Clinical Research Priority Programs (KFSP: From basic research to the clinic: Novel tissue engineered skin grafts for Zurich) of the Faculty of Medicine of the University of Zurich. We are particularly grateful to the Fondation Gaydoul and the sponsors of “DonaTissue” (Thérèse Meier and Robert Zingg) for their generous financial support and interest in our work.

**Conflict of interest** The authors declare that they have no conflict of interest.

## References

- Hermanson A, Dalsgaard CJ (1987) Sensory reinnervation and sensibility in skin transplants. *Med Biol* 65(1):49–52
- Altun V, Hakvoort TE, van Zuijlen PP, van der Kwast TH, Prens EP (2001) Nerve outgrowth and neuropeptide expression during the remodeling of human burn wound scars. A 7-month follow-up study of 22 patients. *Burns* 27(7):717–722
- Ward RS, Tucket RP, English KB, Johansson O, Saffle JR (2003) Substance P axons and sensory threshold increase in burn-graft human skin. *J Surg Res* 118:154–160
- Nedelec B, Hou Q, Sohbi I, Choiniure M, Beaugregard G, Dykes RW (2005) Sensory perception and neuroanatomical structures in normal and grafted skin of burn survivors. *Burns* 31:817–830
- Anderson JR, Zorbas JS, Phillips JK, Harrison JL, Dawson LF, Bolt SE, Rea SM, Klatt JE, Paus R, Zhu B, Giles NL, Drummond PD, Wood FM, Fear MW (2010) Systemic decreases in cutaneous innervation after burn injury. *J Investig Dermatol* 130:1948–1951
- Anderson JR, Fear MW, Phillips JK, Dawson LF, Wallace H, Wood FM, Rea SM (2011) A preliminary investigation of the reinnervation and return of sensory function in burn patients treated with INTEGRA®. *Burns* 37(7):1101–1108
- Botchkarev VA, Eichmuller S, Johansson O, Paus R (1997) Hair cycle-dependent plasticity of skin and hair follicle innervation in normal murine skin. *J Comp Neurol* 386(3):379–395
- Gagnon V, Larouche D, Parenteau-Bareil R, Gingras M, Germain L, Berthod F (2011) Hair follicles guide nerve migration in vitro and in vivo in tissue-engineered skin. *J Investig Dermatol* 131(6):1375–1378
- Carmeliet P, Tessier-Lavigne M (2005) Common mechanisms of nerve and blood vessel wiring. *Nature* 436(7048):193–200
- Carmeliet P (2003) Blood vessels and nerves: common signals, pathways and diseases. *Nat Rev Genet* 4(9):710–720
- Glebova NO, Ginty DD (2005) Growth and survival signals controlling sympathetic nervous system development. *Annu Rev Neurosci* 28:191–222
- Marko SB, Damon DH (2008) VEGF promotes vascular sympathetic innervation. *Am J Physiol Heart Circ Physiol* 294(6):H2646–H2652
- Honma Y, Araki T, Gianino S, Bruce A, Heuckeroth R, Johnson E (2002) Artemin is a vascular-derived neurotrophic factor for developing sympathetic neurons. *Neuron* 35(2):267–282
- Long JB, Jay SM, Segal SS, Madri JA (2009) VEGF-A and Semaphorin3A: modulators of vascular sympathetic innervation. *Dev Biol* 334(1):119–132
- Chauvet S, Burk K, Mann F (2013) Navigation rules for vessels and neurons: cooperative signaling between VEGF and neural guidance cues. *Cell Mol Life Sci* 70(10):1685–1703
- Biedermann T, Böttcher-Haberzeth S, Klar AS, Pontiggia L, Schiestl C, Meuli-Simmen C, Reichmann E, Meuli M (2013)

- Rebuild, restore, reinnervate: do human tissue engineered dermo-epidermal skin analogs attract host nerve fibers for innervation? *Pediatr Surg Int* 29(1):71–78
17. Biedermann T, Pontiggia L, Böttcher-Haberzeth S, Tharakan S, Braziulis E, Schiestl C, Meuli M, Reichmann E (2010) Human eccrine sweat gland cells can reconstitute a stratified epidermis. *J Investig Dermatol* 130(8):1996–2009
  18. Böttcher-Haberzeth S, Biedermann T, Pontiggia L, Braziulis E, Schiestl C, Hendriks B, Eichhoff OM, Widmer DS, Meuli-Simmen C, Meuli M, Reichmann E (2013) Human eccrine sweat gland cells turn into melanin-uptaking keratinocytes in stratifying dermo-epidermal skin substitutes. *J Investig Dermatol* 133(2):316–324
  19. Kiowski G, Biedermann T, Widmer DS, Civenni G, Burger C, Dummer R, Sommer L, Reichmann E (2012) Engineering melanoma progression in a humanized environment in vivo. *J Investig Dermatol* 132(1):144–153
  20. Schneider J, Biedermann T, Widmer D, Montaña I, Meuli M, Reichmann E, Schiestl C (2009) Matriderm versus integra: a comparative experimental study. *Burns* 35(1):51–57
  21. Böttcher-Haberzeth S, Biedermann T, Schiestl C, Hartmann-Fritsch F, Schneider J, Reichmann E, Meuli M (2012) Matriderm® 1 mm versus Integra® Single Layer 1.3 mm for one-step closure of full thickness skin defects: a comparative experimental study in rats. *Pediatr Surg Int* 28(2):171–177
  22. Martin P, Lewis J (1989) Origins of the neurovascular bundle: interactions between developing nerves and blood vessels in embryonic chick skin. *Int J Dev Biol* 33(3):379–387
  23. Quaegebeur A, Lange C, Carmeliet P (2011) The neurovascular link in health and disease: molecular mechanisms and therapeutic implications. *Neuron* 71(3):406–424
  24. Mukoyama YS, Shin D, Britsch S, Taniguchi M, Anderson DJ (2002) Sensory nerves determine the pattern of arterial differentiation and blood vessel branching in the skin. *Cell* 109(6):693–705
  25. Ruiz de Almodovar C, Lambrechts D, Mazzone M, Carmeliet P (2009) Role and therapeutic potential of VEGF in the nervous system. *Physiol Rev* 89(2):607–648
  26. Eichmann A, Thomas JL (2013) Molecular parallels between neural and vascular development. *Cold Spring Harb Perspect Med* 3(1):a006551
  27. Hendrix S, Picker B, Liezmann C, Peters EM (2008) Skin and hair follicle innervation in experimental models: a guide for the exact and reproducible evaluation of neuronal plasticity. *Exp Dermatol* 17(3):214–227
  28. Blais M, Parenteau-Bareil R, Cadau S, Berthod F (2013) Concise review: tissue-engineered skin and nerve regeneration in burn treatment. *Stem Cells Transl Med* 2(7):545–551
  29. Caissie R, Gingras M, Champigny MF, Berthod F (2006) In vivo enhancement of sensory perception recovery in a tissue-engineered skin enriched with laminin. *Biomaterials* 27(15):2988–2993
  30. Blais M, Grenier M, Berthod F (2009) Improvement of nerve regeneration in tissue-engineered skin enriched with Schwann cells. *J Investig Dermatol* 129(12):2895–2900